UvA-DARE (Digital Academic Repository)

Removal of polar organic micropollutants by mixed-matrix reverse osmosis membranes

Albergamo, V.; Blankert, B.; van der Meer, W.G.J.; de Voogt, P.; Cornelissen, E.R.

Removal of polar organic micropollutants by mixed-matrix reverse osmosis membranes

V. Albergamo[a], B. Blankert[b,c], W.G.J. van der Meer[b,d], P. de Voogt[a,e], E.R. Cornelissen[e,f,g,*]

[a] *IBED, University of Amsterdam, Science Park 904, 1098XH Amsterdam, the Netherlands*
[b] *Oasen, Nieuwe Gouwe O.Z. 3, 2801 SB Gouda, the Netherlands*
[c] *Water Desalination and Reuse Center, King Abdullah University of Science and Technology, Thuwal 23955-6900, Saudi Arabia*
[d] *Membrane Science and Technology Group, University of Twente, 7500 AE Enschede, the Netherlands*
[e] *KWR, Water Research Institute, Groningenhaven 7, 3433 PE Nieuwegein, the Netherlands*
[f] *Singapore Membrane Technology Centre, Nanyang Environment and Water Research Institute, Nanyang Technological University, Singapore 637141, Singapore*
[g] *Particle and Interfacial Technology Group, Ghent University, B-9000 Ghent, Belgium*

A B S T R A C T

Mixed-matrix reverse osmosis (RO) membranes have been proposed to outperform standard polyamide thin-film composite (TFC) membranes for the production of high-quality drinking water. We investigated the passage of 30 persistent polar micropollutants (MPs) in a pilot-scale RO system equipped with a 4-inch zeolite-embedded thin-film nanocomposite (TFN) membrane fed with raw riverbank filtrate. Additionally, MPs passage was investigated in a bench-scale system equipped with a 1.8-inch aquaporin-embedded RO membrane. Benchmark TFC membranes were used in both systems. In pilot-scale RO, MPs passage did not exceed 15% and 6% with the TFC and TFN membranes, respectively. In bench-scale RO, MPs passage values of up to 65% and 44% were quantified for the aquaporin and TFC membranes, respectively, suggesting a more open structure of the 1.8-inch modules. In both RO systems, uncharged polar MPs displayed the highest passage values. While neutral MPs of molecular weight lower than 150 Da were better removed by the TFN membrane in pilot-scale RO and by the TFC membrane in bench-scale RO, no substantial differences between passage values of other MPs were observed. Overall, this indicated that nanocomposite and biomimetic membranes are as effective as TFC membranes of the same module size in preventing breakthrough of polar organics.

1. Introduction

Organic micropollutants (MPs) occur ubiquitously in natural waters [1]. Of particular concern for the quality of drinking water sources and finished drinking water is the polar (hydrophilic) fraction of these contaminants. Polar organics can preferentially partition into the water phase, exhibiting high mobility within the water cycle and passing the barriers enforced for drinking water treatment [2]. Links between exposure to trace concentrations of polar MPs and disruption of biological functions of aquatic biota have emerged [3,4], raising concern over the adverse effects of insufficiently treated drinking water to human health [5,6].

It is estimated that by 2025 1.8 billion people will inhabit areas affected by water scarcity and about two-thirds of the world's population will live in water-stressed regions as a result of the cumulative effect of water use, population growth, and climate change [7]. Advanced water treatment processes relying on osmotic membranes are employed by drinking water utilities to cope with the dramatic increase in clean potable water demand. In particular, reverse osmosis (RO) has shown great potential to remove a wide range of contaminants from a

variety of water matrices [8,9] and proved effective in eliminating toxic pollutants in drinking water applications [10]. However, RO produces a waste stream in which the removed (organic) solutes are concentrated as a result of the filtration process, *i.e.* the RO concentrate. From an environmental perspective, this may be considered a limitation of RO and, if not required by law, adequate treatment of concentrate streams should be considered prior to discharge into natural water bodies.

The passage of solutes through RO membranes is assumed to follow the solution-diffusion model, where solutes dissolve into the membrane's active layer, *i.e.* the outermost polymeric layer responsible for solute separation, and diffuse through it along a transmembrane chemical potential gradient [11,12]. The solution-diffusion process can be promoted or hindered by various mechanisms, *i.e.* size exclusion [13,14], electrostatic attraction or repulsion [15,16] and hydrophobic interactions [17,18]. These mechanisms are in turn influenced by the physicochemical properties of both membrane and solutes, feed water composition and RO operating conditions [19,20].

Nowadays the most-sold RO membranes are thin-film composite (TFC) membranes constructed in spiral-wound module configuration [21–23]. A typical TFC membrane consists of three layers, the

outermost active layer being in contact with the feed solution and typically consisting of cross-linked aromatic polyamide (PA) obtained by interfacial polymerisation of 1,3-benzenediamine and trimesoyl chloride on top of a polysulfone layer, which is in turn supported by a polyester web. PA active layers are selective for water molecules and exhibit a high salt rejection, whereas the layers underneath provide support to the overall structure and increase water fluxes to the permeate side being more hydrophilic than the active layer [22]. Despite PA-based TFC membranes have improved over the last decades in terms of water permeability and salt rejection, performance enhancements are limited by the permeability and selectivity trade-off relationship, *i.e.* increasing water permeability will necessarily result in increased solute passage [24,25]. State-of-the art low-pressure PA-based TFC membranes serve as benchmark for any novel material developed for RO filtration [23]. The simplicity of modifying the interfacial polymerisation process has allowed producing mixed-matrix membranes to pursue enhancements of RO performance, *e.g.* by using organic-inorganic and organic-bioorganic composite active layers [22].

In 2007 the first thin-film nanocomposite (TFN) RO membrane was introduced [26]. This nanotechnology-enhanced membrane featured a nanocomposite thin layer (< 0.2 nm) produced by addition of zeolite nanoparticles during interfacial polymerisation of amino and acid chloride monomers. Zeolites are super-hydrophilic and negatively charged minerals which exhibit a 3-D pore network structure. This network serves as a sieve and it is claimed to provide a preferential flow path for water molecules [26,27]. TFN RO membranes have been reported to exhibit higher hydrophilicity and greater water permeability than TFC membranes, while providing comparable salt rejection [26–30]. Various nanomaterials have been used to manufacture more permeable and fouling-resistant TFN membranes, *e.g.* titanium dioxide [31], silver nanoparticles [32] and carbon nanotubes [33]. These and other nanomaterials embedded in the active layer of TFN membranes are discussed in detail in the scientific literature [22,29].

In the last decade there has been a growing interest in biomimetic materials for water purification, particularly in aquaporin-embedded RO membranes. Aquaporins are a family of integral membrane proteins found in all three kingdoms of life at cellular level [34]. These proteins form a pore structure that allows transport of water molecules driven by an osmotic gradient across biological membranes while rejecting ionic solutes [34,35]. Kumar et al. showed that recombinant aquaporin AqpZ from a strain of *E. coli* remained active when incorporated in lipid vesicles and exhibited permeability higher by more than one order of magnitude compared to TFC RO membranes, highlighting the potential benefits of developing biomimetic membranes for water treatment [36]. Recently, mixed-matrix composite membranes with an organic-bioorganic active layer have been successfully manufactured and marketed. Several bench-scale filtration studies claimed that aquaporin-embedded RO membranes could outperform TFC membranes in terms of water permeability and selectivity while providing comparable salt rejection [37–41].

To verify whether novel mixed-matrix membrane chemistry can outperform TFC chemistry with regard to organic solute removal, the passage behaviour of a set of 30 persistent polar MPs was investigated in RO filtration with nanocomposite and biomimetic membranes . A TFN membrane was tested with a pilot-scale RO system, where filtration was applied to a raw riverbank filtrate. Its performance was compared to that of a benchmark TFC membrane. To the best of our knowledge, this is the first study in which a commercially available TFN membrane was used in stand-alone RO drinking water treatment applied to a raw natural water. Additionally, we characterised water permeability, salt rejection and organic solute passage with an aquaporin-based biomimetic membrane in bench-scale RO filtration. The aquaporin RO membrane performance was compared to that of a benchmark TFC membrane. No previous studies have attempted quantifying the passage of an extended set of polar MPs through biomimetic RO membranes. The filtration experiments with aquaporin RO

membrane included two novel pollutants, *i.e.* trifluoromethanesulfonic acid (TFMSA) and 2-(Heptafluoropropoxy)-2,3,3,3-tetrafluoropropionic acid (HFPO-DA). These chemicals are emerging contaminants with high societal relevance. TFMSA, a super acid used in industrial applications, was only recently reported as a ubiquitous water cycle contaminant [42]. HFPO-DA, a chemical introduced to replace perfluorooctanoic acid after the latter was found to be persistent, bioaccumulative and toxic [43], was recently detected in surface waters impacted by wastewater from fluorinated chemical manufacturing and in the drinking water produced from it [44–46]. Besides being novel in terms of recent discovery in the aquatic environment, both TFMSA and HFPO-DA have not yet been investigated in RO filtration.

2. Materials and methods

2.1. Standards and chemicals

All chemicals used for this work were of analytical grade. More details are provided in the Supplementary material (S-1). The model polar MPs tested in this study were chosen from scientific literature data using the following selection criteria: amenability for liquid chromatography-mass spectrometry analysis, detection in natural source waters, finished drinking water and RO permeates. The target MPs selection has been previously described in the scientific literature [47]. The list of the polar MPs is shown in Table 1.

2.2. RO membranes

For the pilot-scale filtration experiments, we chose two 4-inch spiral-wound RO membranes for brackish water desalination. The first membrane was the low-pressure RO (LPRO) membrane ESPA2-LD-4040 (Hydranautics, USA). The ESPA2-LD-4040 is a TFC membrane with an active layer of cross-linked aromatic PA. This membrane served as benchmark to assess the performance of the QuantumFlux Qfx-BW75ES (LG NanoH2O, USA), a TFN membrane with an active layer of zeolite-embedded PA.

For the bench-scale filtration experiments, we chose two 1.8-inch spiral-wound tap water RO membranes. We tested the AQPRTW-1812/150 (Aquaporin A/S, Denmark), a biomimetic RO membrane with a PA active layer embedded with aquaporin protein water channels, and a TW30-1812-100 (DOW Filmtech), the latter serving as a benchmark TFC membrane. It is noteworthy that membrane modules of the same size could not be used in pilot- and bench-scale RO filtration because a 4-inch aquaporin membrane was not commercially available when the experiments were designed. The characteristics of all RO membranes used in the present work are summarised in Table 2.

2.3. RO filtration systems and protocols

2.3.1. Hypoxic RO pilot (4-inch)

A pilot-scale RO system capable of keeping hypoxic conditions in recirculation mode, previously introduced by our research group [47], was used to investigate the removal of polar MPs by 4-inch TFN and TFC membranes. The membranes were tested in separate runs applying the same filtration protocol. The experiments were conducted at a drinking water treatment plant in order to use an actual source water as feed water, *i.e.* raw anaerobic riverbank filtrate. Briefly, the RO pilot consisted of an airtight stainless steel feed water reservoir (720 L) connected to a nitrogen supply, an immersed stainless steel coil fed with cooling liquid from a Chilly 35 AC (Hyfra, Germany), a DPVSV 2/26 B high-pressure pump with frequency-controlled high-speed motor (DP-Pumps, The Netherlands) and one 4-inch membrane pressure vessel. A schematic diagram of the pilot system is given in Fig. 1.

The feed reservoir was filled with approximately 700 L of freshly abstracted anaerobic riverbank filtrate while being flushed with nitrogen. Quality parameters of the feed water measured before dosing

Table 1

List of model polar MPs and their physicochemical properties.

Compound	Molecular weight (Da)	pKa (pKb)[a]	logD (pH 7)[a]	Charge	Chemical classification
1H-benzotriazole	119.05	8.6	1.3	Neutral	Industrial chemical
2,6-Dichlorobenzamide	188.97	12.1	2	Neutral	Biodegradation product
6-Hydroxyquinoline	145.06	10.6	1.8	Neutral	Biodegradation product
Atrazine	215.09	15.8	2.2	Neutral	Herbicide
Barbital	184.19	7.5	0.6	Neutral	Pharmaceutical
Bisphenol A	228.29	9.8	4	Neutral	Personal care product
Caffeine	194.19	(−1.2)	−0.5	Neutral	Stimulant
Carbamazepine	236.27	16	2.8	Neutral	Pharmaceutical
Chloridazon	221.04	(−1.8)	1.1	Neutral	Herbicide
DEET	191.13	(−0.9)	2.5	Neutral	Herbicide
Diuron	233.09	13.2	2.5	Neutral	Herbicide
Diglyme	134.18	n/a	−0.32	Neutral	Industrial chemical
Paracetamol	151.16	0.4	1.2	Neutral	Pharmaceutical
Phenazone	188.22	(−0.5)	0.9	Neutral	Pharmaceutical
Phenylurea	136.06	13.8	0.9	Neutral	Industrial chemical
Tolyltriazole	133.15	8.8	1.8	Neutral	Industrial chemical
Triethyl phosphate	182.15	n/a	1.2	Neutral	Industrial chemical
Acesulfame	162.39	3	−1.5	Negative	Sweetener
Bentazon	240.28	3.7	−0.2	Negative	Herbicide
Diclofenac	295.02	4	1.4	Negative	Pharmaceutical
HFPO-DA[b]	330.05	3.8	1.34	Negative	Industrial chemical
PFBA	213.99	1.2	−1.2	Negative	Industrial chemical
PFBS	299.95	−3.3	0.2	Negative	Industrial chemical
PFOA	413.97	−4.2	1.6	Negative	Industrial chemical
Sulfamethazine	278.08	7	0.4	Negative	Pharmaceutical
Sulfamethoxazole	253.05	6.2	0.1	Negative	Pharmaceutical
TFMSA[b]	150.08	−3.43	−1.35	Negative	Industrial chemical
2-(Methylamino)pyridine	108.07	(6.6)	0.7	Positive	Industrial chemical
Tetrabutylammonium	242.46	n/a	1.3	Positive	Industrial chemical
Tetrapropylammonium	186.35	n/a	−0.4	Positive	Industrial chemical

[a] pKa, pKb and log D calculated with Chemaxon (http://www.chemicalize.com).
[b] Tested only with 1.8-inch modules (aquaporin-embedded and TFC RO membranes).

the polar MPs are given in Supplementary material (Table S-2). A 2-L concentrated solution of polar MPs was prepared as described elsewhere [47] and dosed to the feed water with a SMART Digital pump (Grundfos B.V., The Netherlands), resulting in MPs concentration between 10 and 20 μg L^{-1}. Although these feed concentrations are higher than those commonly quantified in natural freshwaters [51,52], scientific literature data indicated that no significant differences in organic solute passage are expected between the ng L^{-1} and low μg L^{-1}

range [53]. RO filtration was carried out at a fixed 15% recovery and permeate flux was set to 25 L m^{-2} h^{-1}. The feed temperature was 14 ± 0.2 °C and the feed pH was 7.0 ± 0.2. It is noteworthy that, while low recovery values are very common to test spiral-wound membranes in once-through mode and in pilot-scale studies [48], full-scale RO plants are operated at higher recovery (e.g., up to 85%), as they rely on several membrane elements in series. Increasing system recovery results in increased organic solute passage [48] and transport

Table 2

Characteristics of the selected spiral-wound RO membranes modules.

	ESPA2-LD-4040	Qfx-BW75ES	TW30-1812-100	AQPRTW-1812/150
Manufacturer	Hydranautics	LG NanoH2O	DOW	Aquaporin A/S
Type	TFC	TFN	TFC	Aquaporin
Active layer chemistry	Polyamide	Zeolite-embedded polyamide	Polyamide	Aquaporin-embedded polyamide
Module size (inch)	4[a]	4[a]	1.8[a]	1.8[a]
Surface active area (m^2)	7.4[a]	7.0[a]	0.46[a]	0.46[a]
pH range	2 – 11[a]	2 – 11[a]	2 – 11[a]	3 – 10[a]
Maximum feed flow (m^3 h^{-1})	3.6[a]	3.6[a]	0.46[d]	0.57[e]
Permeate flow rate (m^3 d^{-1})	7.6[b]	9.5[c]	0.38[d]	0.67[e]
Stabilised salt rejection (%)	99.6[b]	99.5[c]	90[d]	96[e]
Molecular weight cut-off (Da)	100 – 200[f,g,h]	N/A	N/A	N/A
Contact angle (º)	25 – 40[i]	N/A	N/A	N/A
ζ-Potential at pH 7 (mV)	-25[i]	N/A	N/A	N/A
Surface roughness (nm)	89[i]	N/A	N/A	N/A

NA: not available.
[a] Manufacturer data.
[b] Test conditions: 1500 ppm NaCl solution at 25 °C, 150 psi (10.3 bar), 15% recovery, pH 6.5–7.
[c] Test conditions: 2000 ppm NaCl solution at 25 °C, 150 psi (10.3 bar), 15% recovery, pH 7.
[d] Test conditions: 250 ppm softened tap water at 25 °C, 50 psi (3.4 bar).
[e] Test conditions: 250 ppm softened tap water at 25 °C, 60 psi (4.1 bar).
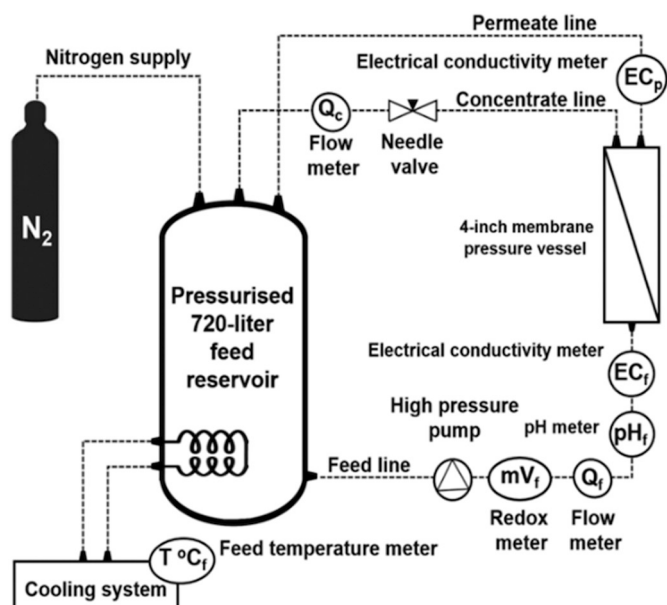[f] [48].
[g] [47].
[h] [49].
[i] [50].

Fig. 1. Schematic diagram of the hypoxic pilot-scale RO system.

models to calculate the impact of recovery on organic solute passage are available in the scientific literature [54]. Filtration was conducted for 4d before taking feed and permeate samples at t = 96 h to ensure equilibration of solute-membrane affinity interactions and avoid over-estimating the passage of moderately hydrophobic MPs [17]. The feed reservoir was supplied with nitrogen during sampling to minimise intrusion of atmospheric oxygen, which would result in precipitation of the dissolved iron naturally occurring in the anaerobic bank filtrate and subsequent fouling of the RO membrane. The stability of the hypoxic conditions of the feed water was assured by an online redox potential meter. Feed water and permeate samples (V = 200 mL; n = 3) were collected in 250 mL polypropylene bottles and frozen immediately on site.

2.3.2. Bench-scale RO (1.8-inch)

The bench-scale RO system consisted of a 500-L feed reservoir equipped with a FC1200 chiller (Julabo GmbH, Germany), a DPVE2–30 frequency controlled pump (DP-Pumps, The Netherlands) and a concentrate valve to regulate the feed flow and pressure. Three parallel lines allowed simultaneous filtration with different RO membranes and recirculation of permeate and concentrate lines to the feed reservoir. Two lines were used and equipped with a 1.8-inch TFC membrane and a 1.8-inch aquaporin membrane, respectively. The feed flow of each line was monitored by built-in rotamers. The feed pressure was monitored by a WIKA 342.11.250 precision pressure gauge (WIKA, Germany). The permeate flow was determined by weighing RO permeate collected in a glass cylinder over an exact 30-s time window prior to each sampling events, i.e. at t = 1 h, t = 48 h, t = 72 h and t = 96 h. The feed reservoir was filled with 400-L tap water previously filtered with Melt Blown 1 μm filters (van Borselen, The Netherlands). A 20 mg L^{-1} polar MPs stock solution was dosed to the feed water to obtain a MPs feed concentration of approximately 40 μg L^{-1}. TFMSA and HFPO-DA were later added to the MPs stock as their societal relevance became clear after the pilot-scale experiments were conducted [46]. Filtration was carried out applying a feed pressure of 3 bar to obtain a permeate flux of 20 L m^{-2} h^{-1} at 5% recovery for both aquaporin and TFC RO membranes. The feed temperature was 17 ± 0.2 °C and the pH was 6.2 ± 0.1. Feed and permeate samples (V = 50 mL; n = 3) were collected into 50-mL polypropylene falcon tubes after 4 days and kept in the dark at 2 °C prior to analysis for not more than one month. A schematic diagram of the bench-scale RO system is shown in Fig. 2.
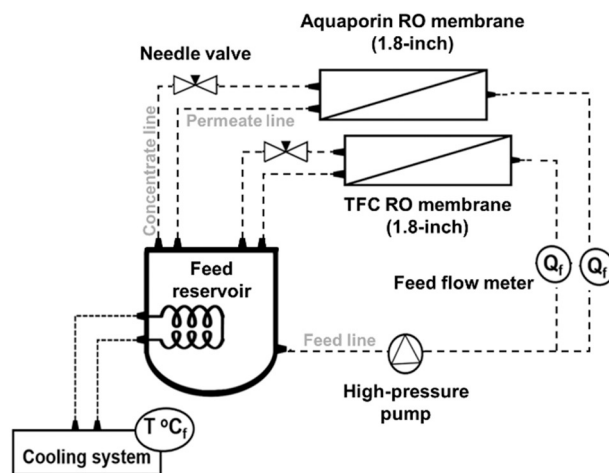

Fig. 2. Schematic diagram of the bench-scale RO system.

2.3.3. Characterisation of 1.8-inch RO membranes

The water permeability of the 1.8-inch aquaporin and TFC RO membranes was characterised for deionised water (DI), DI with 1 g L^{-1} NaCl and tap water using a test procedure routinely applied in-house. The membranes were fitted in parallel pressure vessels and rinsed with DI water in one-pass for 20 min. The system was reverted to re-circulation mode to carry out pure water permeability and salt passage tests. For pure water permeability, a feed pressure of 4 bar at a fixed feed flow of 160 L h^{-1} was applied. Measurements of feed and concentrate pressure as well as permeate flow were taken four times with 1 h interval between each measurement. Further tests involved dosing 1 g L^{-1} of NaCl to the DI water and conducting RO filtration for 1 h without changing operating conditions, i.e. with an applied feed pressure of 4 bar at a fixed feed flow of 160 L h^{-1}. For these tests, water permeability, salt passage (expressed as EC passage), and solute permeability were determined by single measurements. Finally, DI was replaced with locally available low-dissolved organic carbon (DOC) tap water as this was the feed type chosen to assess MPs passage. This tap water is produced from anaerobic groundwater, treated by aeration and rapid sand filtration and distributed without disinfectant residual. Filtration was carried out applying a feed pressure of 3 bar at a feed flow of 160 L h^{-1} and the system was run for 94 h. Water permeability was determined 1 h after starting RO filtration and subsequently at t = 48 h, t = 72 h and t = 96 h. EC passage and solute permeability were instead quantified by single measurements at the beginning and at the end of the experiment, i.e. at t = 1 h and t = 96 h of RO filtration.

2.4. Chemical analysis

2.4.1. Inorganic analysis

Analysis of inorganics in the riverbank filtrate (feed water of hypoxic RO pilot) was performed by Vitens Laboratory (Utrecht, The Netherlands). Chloride, ammonium, phosphate and sulphate were measured by spectrophotometry using a method conforming to the ISO 15923-1:2013 standard. Sodium, potassium, calcium, magnesium, iron and manganese were measured by inductively coupled plasma mass spectrometry using a method conforming to the ISO 17294-2:2016 standard. Hydrogen carbonate was measured by titration using an in-house method. Feed water and RO permeate pH and electrical conductivity were analysed at KWR Water Research Institute (Nieuwegein, The Netherlands) with a Radiometer PHM210 and a Radiometer CDM83, respectively (both by Hach Lange BV, The Netherlands).

2.4.2. Organic analysis

Aliquots of 1 mL feed water and RO permeate from samples taken as described in Sections 2.3.1 and 2.3.2 for the pilot-scale and bench-scale

RO, respectively, were spiked with a mixture of isotope-labelled internal standards to obtain a concentration of 2 μg L^{-1}. The aliquots were filtered with a 0.22 μm polypropylene filters (by Filter-Bio, China) and collected in 1.5 mL polypropylene vials. The samples were analysed by liquid chromatography high-resolution mass spectrometry (LC-HRMS) adopting a direct injection method validated for riverbank filtrate and surface water [55]. The method relied on an ultrahigh-performance Nexera LC system (Shimadzu, Japan) equipped with a core-shell Kinetex biphenyl column (Phenomenex, USA) with a particle size of 2.6 μm, inner diameter of 100 Å and dimensions of 100 × 2.1 mm. The mobile phase eluents were DI 0.05% acetic acid (A) and methanol (B). A maXis 4G quadrupole time-of-flight HRMS (Bruker Daltonik GmbH, Germany) equipped with an electrospray ionisation source was operated in positive and negative mode to achieve MS detection. Unambiguous identification of the MPs was based on the mass accuracy of full-scan HRMS spectra and MS/MS spectra acquired in broadband collision induced dissociation mode (bbCID), LC retention time (t_R) and isotopic fit. The screening parameters for the model target analytes are provided in Table S-3.1, whereas the recoveries and limits of detection and quantification for direct injection analysis of riverbank filtrate and RO permeate are provided in Table S-3.2. It is noteworthy that while a validation study for the analysis of tap water (bench-scale RO feed water) was not performed, the robustness and applicability of direct injection analysis to other water matrices has been previously shown [55]. Hence, even if uncharacterised matrix effects may occur in tap water, the measurements of the bench-scale RO feed water (n = 4) are considered reliable to compare the TFC and aquaporin RO membranes, which were fed in parallel in the bench-scale system. A separate chromatographic method was needed for the analysis of TFMSA. LC separation of TFMSA was achieved on an Acclaim Mixed-Mode WAX-1 column with a particle size of 3 μm, inner diameter of 120 Å and dimensions of 3.0 × 50 mm (Thermo Fisher, USA). The mobile phase eluents were DI (A) and methanol (B), both 5 mM ammonium acetate. A 10-min linear gradient at 90% B and a flow of 0.3 mL/min were used. The sample injection volume was 80 μL.

2.5. Assessment of solute passage

The following equation was used to calculate the passage of solutes by RO membranes:

$$P\,(\%) = (C_{ROP}/C_{ROF}) \times 100 \qquad (1)$$

where C_{ROP} and C_{ROF} are the concentrations in the permeate and the feed water, respectively.

The EC passage was calculated as:

$$EC\,P\,(\%) = (EC_{ROP}/EC_{ROF}) \times 100 \qquad (2)$$

where EC_{ROP} and EC_{ROF} are the electrical conductivity (in μS/cm) in the permeate and the in the bulk feed solution, respectively.

Based on the solution-diffusion model the water permeability (A) of RO membranes was calculated by rearranging the permeate flux equation [11,12]:

$$J_W = A\,(\Delta P - \Delta\Pi) \qquad (3)$$

where J_W is the permeate flux (in L m^{-2} h^{-1}), ΔP and $\Delta\Pi$ indicate the pressure and osmotic pressure difference across the membrane, respectively.

Similarly, the solute permeability (B) was calculated as:

$$B = J_W\,(C_{ROP}/C_{ROF} - C_{ROP}) \qquad (4)$$

3. Results and discussion

3.1. Hypoxic pilot-scale RO

3.1.1. TFN and TFC RO membranes performance (4-inch)

In a previous work conducted with the same RO pilot it was shown that the physicochemical properties of the MPs were significantly related to passage rate through TFC membranes [47]. These properties were specifically size and charge, whereas hydrophobicity did not show statistical significance difference compared to hydrophilicity. Hence, based on these earlier findings and on other literature data, all neutral MPs are discussed together and separately from ionic MPs.

At the moment of sampling, the TFN membrane displayed a water permeability of 1.22 L m^{-2} h^{-1} bar^{-1} and an EC passage of 1.2%, whereas the TFC membrane showed a water permeability of 1.95 L m^{-2} h^{-1} bar^{-1} and an EC passage of 0.9%. At a fixed feed flow of ≈ 1 m^3 h^{-1} the TFN membrane required a feed pressure of 19.55 bar to match the set operating conditions, while the TFC membrane needed 13.35 bar. This was not in line with literature data, based on which a higher water permeability of TFN membranes was expected (*cf.* Section 1. Introduction). A lower permeability of the TFN membrane due to compaction was ruled out, as zeolite-embedded polyamide active layers are reportedly less prone to undergo such modifications [30]. Hofs et al. showed that a 4-inch seawater QuantumFlux TFN membrane outperformed a benchmark TFC membrane in water permeability by a factor of 2 in pilot-scale RO applied to tap water with 1 g L^{-1} NaCl at a permeate flux of 15 L m^{-2} h^{-1} and 7% recovery [28]. That study found that the TFN membrane was less hydrophilic compared to the TFC membrane based on contact angle measurements. The TFN membrane's lower permeability observed in our study might be supported by this finding. While Hofs et al. used filtered tap water, we used raw riverbank filtrate as RO feed water. DOC naturally occurs in this riverbank filtrate at a concentration of approximately 8 mg L^{-1} [56]. Therefore, it could be speculated that the TFN membrane might have exhibited higher affinity for the hydrophobic fraction of the feed water DOC, which led to reduced water and solute permeability [57–59]. However, flux decline or membrane autopsy data to support this statement are not available.

3.1.2. Removal of neutral MPs by hypoxic RO pilot (4-inch)

The removal of neutral MPs expressed as compound passage though the TFN membrane and the benchmark TFC membrane is shown in Fig. 3a. The passage profiles of neutral polar MPs followed a similar trend. The TFN membrane, however, proved to be a more effective barrier against neutral polar MPs, for which passage values between 0.1% and 6.1% were quantified. These values ranged from 0.1% to 14.7% when filtration was carried out with the benchmark TFC membrane. The TFN membrane was more effective in rejecting neutral polar MPs of molecular weight lower than 150 Da and comparable to the TFC membrane for larger neutral MPs. The only exception was the plasticiser bisphenol A, a neutral polar organic with a log D_{pH7} of 4, thus exhibiting hydrophobic properties. Bisphenol A displayed 4.2 ± 2.6% and 1.8 ± 0.3% passage through the TFN and TFC RO membranes, respectively. Its incomplete removal by low-pressure TFC RO membranes has been reported before by our research group [47] and in the literature [60]. This passage behaviour may result from affinity interactions with the hydrophobic membrane active layer, ultimately enhancing the solution-diffusion mechanism [61,62]. The higher passage of bisphenol A through the TFN membrane could be supported by the higher hydrophobicity of the QuantumFlux nanocomposite as measured by Hofs et al. [28]. In order of size expressed as molecular weight, the smallest neutral polar MPs were 1H-benzotriazole (119.12 Da) < tolyltriazole (133. 15 Da) < diglyme (134.17 Da) < phenylurea
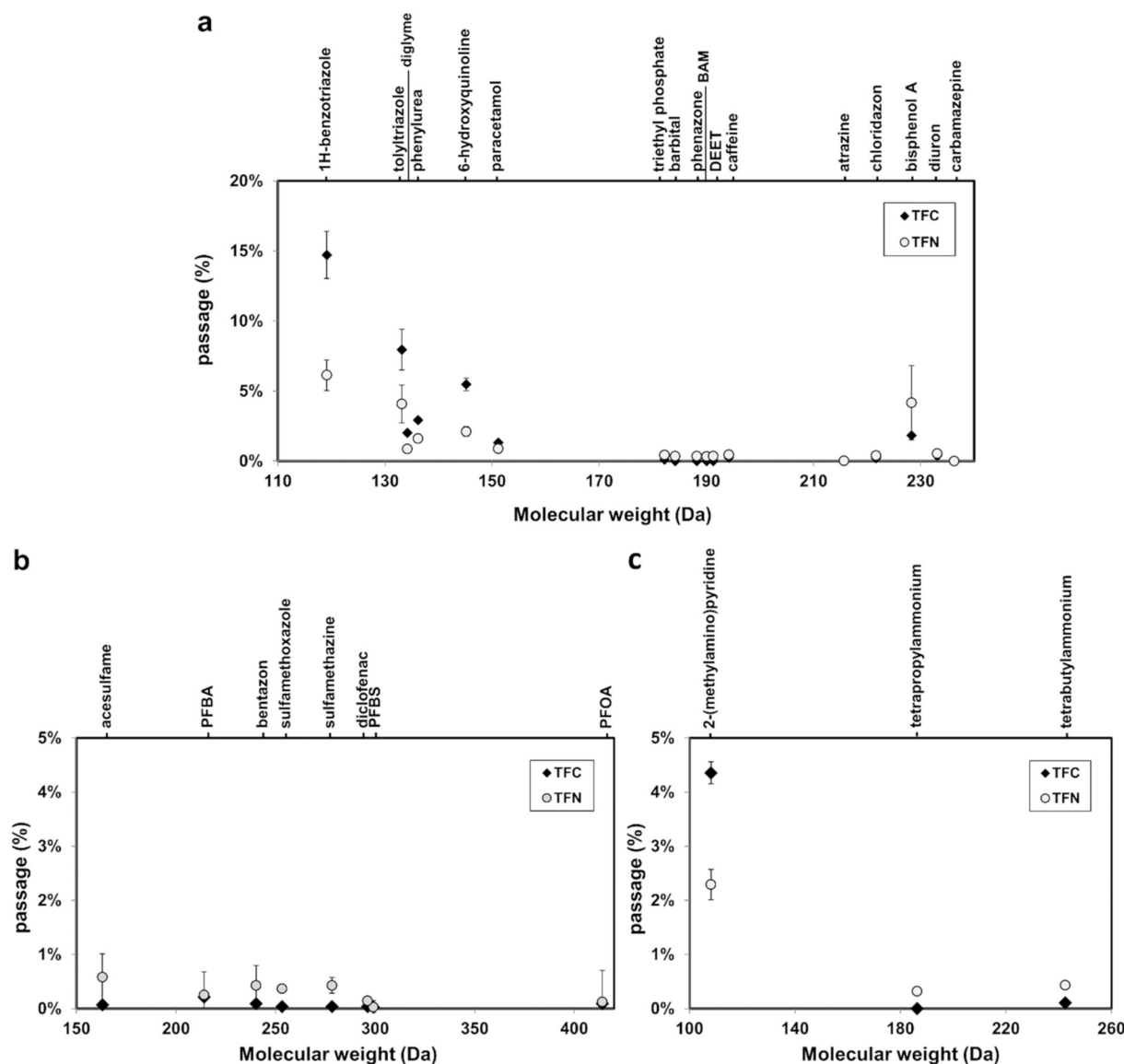
Fig. 3. Passage of neutral polar MPs (a), anionic MPs (b) and cationic MPs (c) through TFN and TFC membranes as a function of compound molecular weight. Error bars are shown when larger than the data point symbol and indicate the standard deviation of the measurements for n = 3 samples. Conditions: average permeate flux 25 L m^{-2} h^{-1}, recovery 15%, feed pH 7.0 ± 0.2, feed conductivity 973 ± 7 μS/cm, feed temperature 14 ± 0.2 °C.

(136.15 Da) < 6-hydroxyquinoline (145.16 Da). As expected, 1H-benzotriazole displayed the highest passage through the TFC and TFN RO membranes with values of 14.7 ± 1.7% and 6.1 ± 1.1%, respectively. The second least-removed MP was tolyltriazole, which displayed passage values of 8.0 ± 1.5% and 4.1 ± 1.4% with the TFC and TFN RO membranes, respectively. The third least-removed MP was 6-hydroxyquinoline with passage values of 5.5 ± 0.4% and 2.1 ± 0.4% with the TFC and TFN RO membranes, respectively. Overall the passage-size profile displayed by neutral polar MPs was in accordance with literature data for both the TFC [48] and the TFN RO membranes [28]. Hofs et al. investigated the removal of 8 neutral nitrosamines and 21 pharmaceuticals including neutral and ionic compounds by TFN and TFC membranes [28]. While both membranes achieved excellent rejections of pharmaceuticals (> 99%), most nitrosamines were well rejected (> 90%) according to their molecular weight. NDMA, the smallest nitrosamine with a molecular weight of 74.1 Da, was rejected for ≈ 62% and ≈ 74% by the TFN and the TFC RO membranes, respectively. This was partially in accordance with our results, as we also observed a higher passage for the smallest neutral MPs, but in our case the TFN membrane exhibited lower passage values.

It is challenging to thoroughly compare our study to that of Hofs et al. as we used a raw natural water as RO feed, whereas they used filtered tap water, which is a much simpler matrix, thus less likely to cause fouling and affect the membrane performance. Considering that similar removal patterns were exhibited by the 4-inch membrane modules tested with the RO-pilot, and that the TFN membrane's nanoparticle load is estimated to be below 6 wt% [28], it could be assumed that separation of organic solutes by nanocomposite active layers followed a solution-diffusion mechanism through PA.

3.1.3. Removal of ionic MPs by hypoxic RO pilot (4-inch)

The passage of anionic MPs through TFN and TFC RO membranes is shown in Fig. 3b. Excellent removal of negatively charged organic solutes was observed for both membranes and passage values lower than 1% were quantified in all cases. These MPs bore a negative charge because of deprotonation of acidic functional groups along their structures, which had pKa values lower than the feed water pH. Likewise, it could be assumed that both membranes would exhibit a negative charge at feed water pH due to deprotonation of acidic functional groups on the polyamide (nano)composite [14,19,29]. Literature data

supported this assumption as no zeta-potential differences were observed between a QuantumFlux TFN and a benchmark TFC RO membranes [28]. Electrostatic repulsion with negatively charged RO membranes prevents anionic MPs from dissolving into the active layer [15,16], representing a strong factor enhancing removal by RO regardless of other MPs structural properties.

Good removal of cationic MPs was provided by both membranes tested with the hypoxic RO pilot, with passage values lower than 5% in all cases (Fig. 3c). The TFN membrane proved to be a more effective barrier against the smallest cationic MP, *i.e.* 2-(methylamino)pyridine (109.08 Da), for which 2.3 ± 0.3% passage was quantified *versus* 4.3 ± 0.2% passage through the TFC membrane. In this case, the better performance of the TFN might be attributed to the cation exchange capacity of zeolites nanoparticles embedded in nanocomposite films [63]. 2-(methylamino)pyridine was the smallest compound investigated in this study, nevertheless it displayed lower passage than the second-smallest 1H-benzotriazole (119.12 Da), which was uncharged instead. This indicated that additional solute-membrane interactions, likely electrostatic, prevent small cationic MPs to dissolve and diffuse through negatively charged (nano)composite resulting in a lower passage compared to neutral MPs of similar size. The organic ammonium cations were slightly better removed by the TFC membrane, nevertheless passage values lower than 0.5% were quantified for tetrapropylammonium and tetrabutylammonium in all cases. For cationic MPs, in addition to size exclusion, electrostatic sorption [16,48] and Donnan exclusion [64] are expected to play a role in preventing chemical passage through RO membranes.

3.2. Bench-scale RO (1.8-inch)

3.2.1. Aquaporin and TFC RO membranes performance

Water permeability (A), salt passage, solute permeability (B) and trade-off (A/B) of the 1.8-inch aquaporin and benchmark TFC RO membranes are presented in Table 3. When DI water was used as feed water, the aquaporin membrane was more permeable than the TFC by 33–35%. The higher permeability of the aquaporin membrane ($A_{aquaporin}$ = 10.22 ± 0.03 L m^{-2} h^{-1} bar^{-1}) compared to that of the benchmark TFC membrane (A_{TFC} = 7.63 ± 0.12 L m^{-2} h^{-1} bar^{-1}) might have resulted from the water-selective protein channels embedded in the bioorganic composite, although a less dense membrane structure could not be ruled out. Upon checking the stability of the filtration performance over 4 h, NaCl was added to the DI water to a concentration of 1 g L^{-1}. In these conditions, water permeability of the aquaporin membrane decreased by 37%, whereas the TFC membrane displayed a decrease of 26%. The TFC displayed salt passage and solute permeability (B) higher than those of the aquaporin membrane by nearly a factor of 2 while exhibiting half of the trade-off value (A/B). This indicated the higher permeability of the aquaporin RO membrane

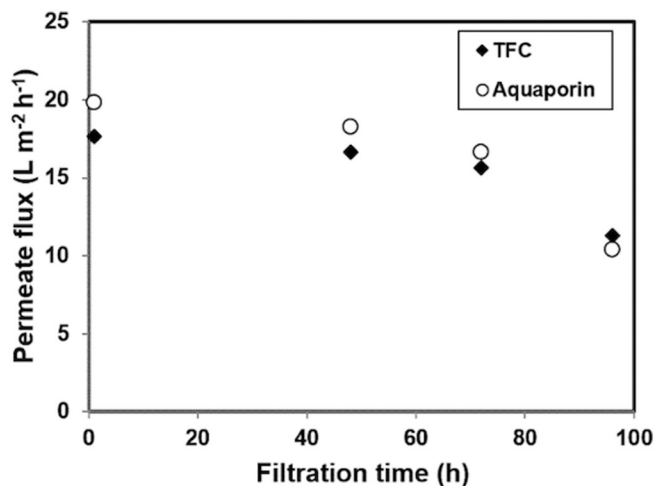**Fig. 4.** Flux decline expressed as permeate flux (L m^{-2} h^{-1}) over time (h) of the aquaporin and TFC membranes in bench-scale RO filtration.

to water molecules and lower selectivity for monovalent ions in high salinity conditions. No substantial differences in the evaluated performance parameters were observed between the aquaporin and TFC membranes over 96 h of RO filtration when tap water was used as feed water. This was in contrast with the performance data reported in the manufacturer datasheets, where the stabilised salt rejection of the aquaporin membrane was 96% and that of the TFC membrane was 90% (as shown in Table 2). In addition, the two membranes displayed a comparable flux decline over time, as shown in Fig. 4.

3.2.2. Removal of neutral MPs in bench-scale RO (1.8-inch)

The passage of neutral MPs through aquaporin and benchmark TFC RO membranes is shown in Fig. 5a. Results for barbital, atrazine and bisphenol A are not shown as the concentrations in the feed water decreased below their quantification limits. While this phenomenon has been reported before for other MPs and attributed to adsorption onto the membrane surface [65], we believe that in our case adsorption onto the feed reservoir and pipelines of the bench-scales RO system has occurred. Adsorption onto the membrane surface may be ruled out as this phenomenon was not observed in pilot-scale RO filtration.

The order in which the neutral MPs were removed by the 1.8-inch membranes was similar to that observed in pilot-scale RO filtration, although the passage of uncharged polar MPs smaller than 150 Da was higher in bench-scale. For example, while 1H-benzotriazole displayed 14.7 ± 1.7% with the 4-inch TFC membrane, values of 44 ± 4% and 65 ± 10% were quantified for the 1.8-inch TFC and the aquaporin RO

Table 3
Performance of aquaporin-embedded and benchmark TFC RO membranes (1.8-inch).

		Water permeability (A)	Salt passage	Solute permeability (B)	Trade-off (A/B)
		L m^{-2} h^{-1} bar^{-1}	%	L m^{-2} h^{-1}	bar^{-1}
Aquaporin membrane	DI[a]	10.22 ± 0.03	N/A	N/A	N/A
	DI + NaCl 1 g L^{-1}[b]	6.34	7.01	1.89	3.35
	Tap water	5.43 ± 1.37[c]	2.4 ± 0.4[d]	0.39 ± 0.19[d]	13.92
TFC membrane	DI[a]	7.63 ± 0.12[a]	N/A	N/A	N/A
	DI + NaCl 1 g L^{-1}[b]	5.39[b]	15.52	3.96	1.36
	Tap water	5.10 ± 0.94[c]	2.4 ± 1.1[d]	0.39 ± 0.23[d]	13.07

N/A = not available.

[a] n = 4 (one measurement per hour, value after the ± sign indicates standard deviation of the measurements), feed pressure = 4 bar.

[b] n = 1, feed pressure = 4 bar.

[c] n = 4 (measured at t = 1 h, t = 48 h, t = 72 h and t = 96 h. Value after the ± sign indicates standard deviation of the measurements) and feed pressure = 3 bar.

[d] n = 2 (average of measurements taken at t = 1 h and t = 96 h, value after the ± sign indicates the range of the duplicates).
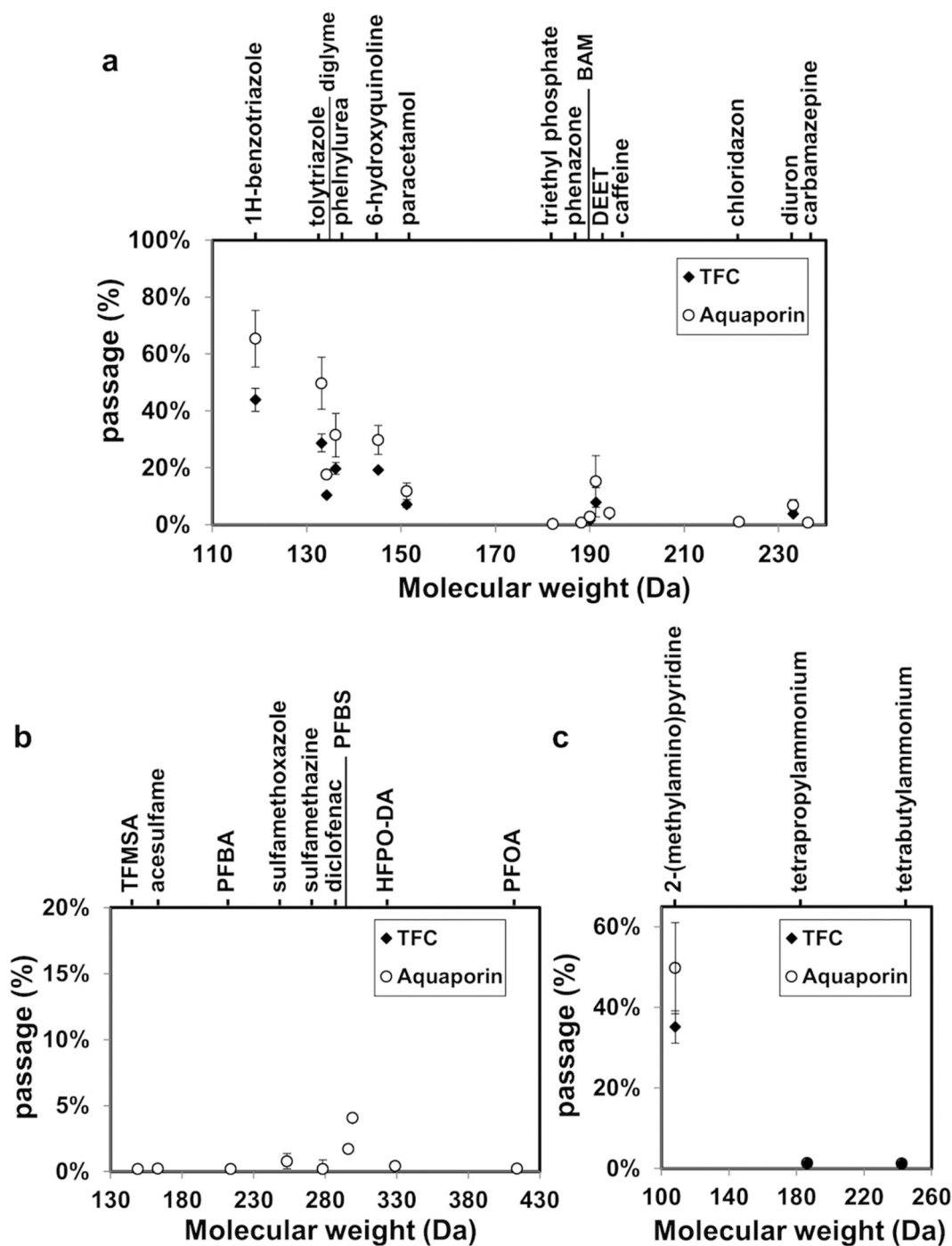
Fig. 5. Passage of neutral polar MPs (a), anionic MPs (b) and cationic MPs (c) through 1.8-inch aquaporin and TFC RO membranes as a function of compound molecular weight. Error bars are shown when larger than the data point symbol and indicate the standard deviation of the measurements for n = 3 samples. Conditions: average permeate flux 20 L m^{-2} h^{-1}, recovery 6%, feed pH 6.2 ± 0.1, feed conductivity 237 μS/cm, feed temperature 17 °C. Symbol overlap indicates that concentrations in the permeate produced by both membranes were below the analytical method's quantification limit.

membranes, respectively. As feed water pH and temperature did not differ substantially between bench-scale (pH 6.2 ± 0.1, T = 17 °C) and pilot-scale (pH 7.0 ± 0.2, T = 14 ± 0.2 °C), the higher passage of neutral MPs and the higher water permeability of the 1.8-inch might have resulted from a more open structure compared to that of the 4-inch RO membranes.

In bench-scale filtration, neutral MPs smaller than 150 Da exhibited higher passage through the aquaporin membrane compared to the TFC membrane. The passage of the five smallest neutral MPs, *i.e.* 1H-benzotriazole (119,12 Da), tolyltriazole (133.15 Da), diglyme (134.18 Da),

phenylurea (136.15 Da) and 6-hydroxyquinoline (145.16 Da) ranged according to size from 44 ± 4% to 19 ± 1% with the TFC membrane, whereas the range for the aquaporin membrane was 65 ± 10% to 30 ± 5%. No differences were observed for larger compounds. Despite evidence of diffusion of small neutral organics and even small peptides through aquaporin water channels exists [66–68], MPs passage is believed to occur mostly through the PA active layer. This was recently confirmed for aquaporin-embedded PA forward osmosis membranes [69]. Unfortunately, further RO studies to compare the results of the aquaporin membrane were not found in the literature.

3.2.3. Removal of ionic MPs in bench-scale RO (1.8-inch)

The passage of ionic MPs through the biomimetic aquaporin and a benchmark TFC membrane is shown in Fig. 5b (anionic) and Fig. 5c (cationic). Variations due to different concentration polarisation conditions were not expected as membrane modules of the same size were used [16] and the operating conditions were similar during the experiments.

Anionic MPs were extremely well removed and exhibited passage values lower than 1% in all cases with both membranes, except PFBS, which displayed 4% passage with both aquaporin and TFC membranes. The reason behind the increased passage of PFBS is currently unclear and needs further investigation. In all cases the quantification limits were used as permeate concentrations, leading to overlapping data points in Fig. 5b. The passage of TFMSA through RO membranes was quantified for the first time in the present study. The method to analyse TFMSA was not validated due to time constraints. Nevertheless, its output was considered reliable on the basis of linearity of the calibration series used for quantification ($R^2 = 0.9986$) and on the standard error of the measured samples ($< 13\%$). TFMSA displayed passage of 0.4% with both membranes, indicating that under-the-tap RO modules (1.8-inch) perform as well as the 4-inch membranes in rejecting small anionic MPs.

As for cationic MPs (Fig. 5c), the ammonium cations displayed < 1.5% passage through both aquaporin and TFC RO membranes. Surprisingly, the smallest cation 2-(methylamino)pyridine displayed passage comparable to that of 1H-benzotriazole with both aquaporin and TFC RO membranes. This data did not reflect the results from pilot-scale RO filtration. As the pilot-scale RO was fed with raw bank filtrate, negatively charged DOC naturally occurring in this feed water might have electrostatically adsorbed cationic MPs [70], resulting in a decreased passage of positively charged organic compounds.

4. Conclusions

Based on the observations from pilot-scale RO filtration applied to a natural water, the following conclusions were made:

- The TFN membrane was a more effective barrier against neutral MPs smaller than 150 Da and comparable for larger molecules, indicating that the zeolite nanoparticles might act as additional sieves. The passage differences between the TFN and TFC membranes became narrower with increasing MPs molecular weight.
- Anionic MPs were extremely well removed by the TFC and TFN membranes (passage values < 1%), indicating that electrostatic interactions prevented solution-diffusion of these chemicals regardless of the presence of embedded additives in the membrane active layer. Cationic MPs were also well removed by both membranes, although the TFN displayed lower passage of the smallest cation. For the three cationic MPs, passage was lower than that of neutral MPs of comparable size, indicating a substantial contribution of electrostatic interactions in preventing passage of small cations.

Based on the observations from bench-scale RO filtration applied to tap water, the following conclusions were made:

- The aquaporin RO membrane was more water-permeable and exhibited a lower EC passage than the benchmark TFC when deionised water was used as feed water, suggesting both higher affinity for water molecules and less affinity for salts. When tap water was used as feed water, higher water permeability resulted in higher organic solute passage, as shown by the permeability-selectivity trade-off, highlighting the different behaviour of salts from that of organics.
- Anionic MPs were extremely well removed by the 1.8-inch modules, proving the efficacy of RO against anionic organics. On the other hand, small cationic MPs were more problematic with the 1.8-inch modules regardless of membrane chemistry.

Our study indicated that while different active layer chemistry can result in different passage values of organic solutes, commercially available nanocomposite and biomimetic RO membranes cannot substantially outperform benchmark TFCs. More research on membrane materials is needed to improve the performance of RO against polar MPs and overcome the limitations posed by the permeability-selectivity relationship trade-off.

CRediT authorship contribution statement

V. Albergamo: Investigation, Formal analysis, Visualization, Writing - original draft, Writing - review & editing. **B. Blankert:** Methodology, Supervision, Writing - review & editing. **W.G.J. van der Meer:** Funding acquisition, Conceptualization, Methodology, Resources, Supervision, Writing - review & editing. **P. de Voogt:** Funding acquisition, Conceptualization, Methodology, Resources, Supervision, Writing - review & editing. **E.R. Cornelissen:** Methodology, Supervision, Resources, Writing - review & editing.

Declaration of competing interest

The authors declare that they have no known competing financial interests or personal relationships that could have appeared to influence the work reported in this paper.

Appendix A. Supplementary data

Supplementary data to this article can be found online at https://doi.org/10.1016/j.desal.2020.114337.

References

[1] R.P. Schwarzenbach, B.I. Escher, K. Fenner, T.B. Hofstetter, C.A. Johnson, U. von Gunten, B. Wehrli, The challenge of micropollutants in aquatic systems, Science 313 (2006) 1072–1077 (80-.), http://science.sciencemag.org/content/313/5790/1072.abstract.

[2] T. Reemtsma, U. Berger, H.P.H. Arp, H. Gallard, T.P. Knepper, M. Neumann, J.B. Quintana, P. de Voogt, Mind the gap: persistent and mobile organic compounds—water contaminants that slip through, Environ. Sci. Technol. 50 (2016) 10308–10315, https://doi.org/10.1021/acs.est.6b03338.

[3] T.B. Hayes, V. Khoury, A. Narayan, M. Nazir, A. Park, T. Brown, L. Adame, E. Chan, D. Buchholz, T. Stueve, S. Gallipeau, Atrazine induces complete feminization and chemical castration in male African clawed frogs (Xenopus laevis), Proc. Natl. Acad. Sci. 107 (2010) 4612–4617, https://doi.org/10.1073/pnas.0909519107.

[4] S. Kashiwada, H. Ishikawa, N. Miyamoto, Y. Ohnishi, Y. Magara, Fish test for endocrine-disruption and estimation of water quality of Japanese rivers, Water Res. 36 (2002) 2161–2166, https://doi.org/10.1016/S0043-1354(01)00406-7.

[5] M. Schriks, M.B. Heringa, M.M.E. van der Kooi, P. de Voogt, A.P. van Wezel, Toxicological relevance of emerging contaminants for drinking water quality, Water Res. 44 (2010) 461–476, https://doi.org/10.1016/j.watres.2009.08.023.

[6] E. Diamanti-Kandarakis, J.-P. Bourguignon, L.C. Giudice, R. Hauser, G.S. Prins, A.M. Soto, R.T. Zoeller, A.C. Gore, Endocrine-disrupting chemicals: an Endocrine

Society scientific statement, Endocr. Rev. 30 (2009) 293–342 https://doi.org/10.1210/er.2009-0002.

[7] FAO, Coping with water scarcity - challenge of the twenty-first century, http://www.fao.org/3/a-aq444e.pdf, (2007) , Accessed date: 20 January 2019.

[8] J. Lee, B.C. Lee, J.S. Ra, J. Cho, I.S. Kim, N.I. Chang, H.K. Kim, S.D. Kim, Comparison of the removal efficiency of endocrine disrupting compounds in pilot scale sewage treatment processes, Chemosphere 71 (2008) 1582–1592, https://doi.org/10.1016/j.chemosphere.2007.11.021.

[9] J. Radjenović, M. Petrović, F. Ventura, D. Barceló, Rejection of pharmaceuticals in nanofiltration and reverse osmosis membrane drinking water treatment, Water Res. 42 (2008) 3601–3610, https://doi.org/10.1016/j.watres.2008.05.020.

[10] V. Albergamo, B.I. Escher, E.L. Schymanski, R. Helmus, M.M.L. Dingemans, E.R. Cornelissen, M.H.S. Kraak, J. Hollender, P. de Voogt, Evaluation of reverse osmosis drinking water treatment of riverbank filtrate using bioanalytical tools and non-target screening, Environ. Sci. Water Res. Technol. (2019), https://doi.org/10.1039/C9EW00741E.

[11] J. Wang, D.S. Dlamini, A.K. Mishra, M.T.M. Pendergast, M.C.Y. Wong, B.B. Mamba, V. Freger, A.R.D. Verliefde, E.M.V. Hoek, A critical review of transport through osmotic membranes, J. Memb. Sci. 454 (2014) 516–537, https://doi.org/10.1016/j.memsci.2013.12.034.

[12] J.G. Wijmans, R.W. Baker, The solution-diffusion model: a review, J. Memb. Sci. 107 (1995) 1–21, https://doi.org/10.1016/0376-7388(95)00102-I.

[13] K. Kimura, G. Amy, J.E. Drewes, T. Heberer, T.-U. Kim, Y. Watanabe, Rejection of organic micropollutants (disinfection by-products, endocrine disrupting compounds, and pharmaceutically active compounds) by NF/RO membranes, J. Memb. Sci. 227 (2003) 113–121, https://doi.org/10.1016/j.memsci.2003.09.005.

[14] H. Ozaki, H. Li, Rejection of organic compounds by ultra-low pressure reverse osmosis membrane, Water Res. 36 (2002) 123–130, https://doi.org/10.1016/S0043-1354(01)00197-X.

[15] L.D. Nghiem, A.I. Schäfer, M. Elimelech, Role of electrostatic interactions in the retention of pharmaceutically active contaminants by a loose nanofiltration membrane, J. Memb. Sci. 286 (2006) 52–59, https://doi.org/10.1016/j.memsci.2006.09.011.

[16] A.R.D. Verliefde, E.R. Cornelissen, S.G.J. Heijman, J.Q.J.C. Verberk, G.L. Amy, B. Van der Bruggen, J.C. van Dijk, The role of electrostatic interactions on the rejection of organic solutes in aqueous solutions with nanofiltration, J. Memb. Sci. 322 (2008) 52–66, https://doi.org/10.1016/j.memsci.2008.05.022.

[17] K. Kimura, G. Amy, J. Drewes, Y. Watanabe, Adsorption of hydrophobic compounds onto NF/RO membranes: an artifact leading to overestimation of rejection, J. Memb. Sci. 221 (2003) 89–101, https://doi.org/10.1016/S0376-7388(03)00248-5.

[18] A.R.D. Verliefde, E.R. Cornelissen, S.G.J. Heijman, E.M.V. Hoek, G.L. Amy, B. Van der Bruggen, J.C. van Dijk, Influence of solute−membrane affinity on rejection of uncharged organic solutes by nanofiltration membranes, Environ. Sci. Technol. 43 (2009) 2400–2406, https://doi.org/10.1021/es803146r.

[19] C. Bellona, J.E. Drewes, P. Xu, G. Amy, Factors affecting the rejection of organic solutes during NF/RO treatment—a literature review, Water Res. 38 (2004) 2795–2809, https://doi.org/10.1016/j.watres.2004.03.034.

[20] K.V. Plakas, A.J. Karabelas, Removal of pesticides from water by NF and RO membranes — a review, Desalination 287 (2012) 255–265, https://doi.org/10.1016/j.desal.2011.08.003.

[21] F. Perreault, M.E. Tousley, M. Elimelech, Thin-film composite polyamide membranes functionalized with biocidal graphene oxide nanosheets, Environ. Sci. Technol. Lett. 1 (2014) 71–76, https://doi.org/10.1021/ez4001356.

[22] K.P. Lee, T.C. Arnot, D. Mattia, A review of reverse osmosis membrane materials for desalination—development to date and future potential, J. Memb. Sci. 370 (2011) 1–22, https://doi.org/10.1016/J.MEMSCI.2010.12.036.

[23] R.J. Petersen, Composite reverse osmosis and nanofiltration membranes, J. Memb. Sci. 83 (1993) 81–150, https://doi.org/10.1016/0376-7388(93)80014-O.

[24] G.M. Geise, H.B. Park, A.C. Sagle, B.D. Freeman, J.E. McGrath, Water permeability and water/salt selectivity tradeoff in polymers for desalination, J. Memb. Sci. 369 (2011) 130–138, https://doi.org/10.1016/j.memsci.2010.11.054.

[25] J.R. Werber, A. Deshmukh, M. Elimelech, The critical need for increased selectivity, not increased water permeability, for desalination membranes, Environ. Sci. Technol. Lett. 3 (2016) 112–120, https://doi.org/10.1021/acs.estlett.6b00050.

[26] B.-H. Jeong, E.M.V. Hoek, Y. Yan, A. Subramani, X. Huang, G. Hurwitz, A.K. Ghosh, A. Jawor, Interfacial polymerization of thin film nanocomposites: a new concept for reverse osmosis membranes, J. Memb. Sci. 294 (2007) 1–7, https://doi.org/10.1016/J.MEMSCI.2007.02.025.

[27] M.L. Lind, A.K. Ghosh, A. Jawor, X. Huang, W. Hou, Y. Yang, E.M.V. Hoek, Influence of zeolite crystal size on zeolite-polyamide thin film nanocomposite membranes, Langmuir 25 (2009) 10139–10145, https://doi.org/10.1021/la900938x.

[28] B. Hofs, R. Schurer, D.J.H. Harmsen, C. Ceccarelli, E.F. Beerendonk, E.R. Cornelissen, Characterization and performance of a commercial thin film nanocomposite seawater reverse osmosis membrane and comparison with a thin film composite, J. Memb. Sci. 446 (2013) 68–78, https://doi.org/10.1016/j.memsci.2013.06.007.

[29] W.J. Lau, S. Gray, T. Matsuura, D. Emadzadeh, J. Paul Chen, A.F. Ismail, A review on polyamide thin film nanocomposite (TFN) membranes: history, applications, challenges and approaches, Water Res. 80 (2015) 306–324, https://doi.org/10.1016/J.WATRES.2015.04.037.

[30] M.M. Pendergast, A.K. Ghosh, E.M.V. Hoek, Separation performance and interfacial properties of nanocomposite reverse osmosis membranes, Desalination 308 (2013) 180–185, https://doi.org/10.1016/J.DESAL.2011.05.005.

[31] S.-Y. Kwak, S.H. Kim, S.S. Kim, Hybrid organic/inorganic reverse osmosis (RO) membrane for bactericidal anti-fouling. 1. Preparation and characterization of TiO2

nanoparticle self-assembled aromatic polyamide thin-film-composite (TFC) membrane, Environ. Sci. Technol. 35 (2001) 2388–2394, https://doi.org/10.1021/es0017099.

[32] M. Ben-Sasson, X. Lu, E. Bar-Zeev, K.R. Zodrow, S. Nejati, G. Qi, E.P. Giannelis, M. Elimelech, In situ formation of silver nanoparticles on thin-film composite reverse osmosis membranes for biofouling mitigation, Water Res. 62 (2014) 260–270, https://doi.org/10.1016/j.watres.2014.05.049.

[33] V. Vatanpour, M. Safarpour, A. Khataee, H. Zarrabi, M.E. Yekavalangi, M. Kavian, A thin film nanocomposite reverse osmosis membrane containing amine-functionalized carbon nanotubes, Sep. Purif. Technol. 184 (2017) 135–143, https://doi.org/10.1016/j.seppur.2017.04.038.

[34] P. Agre, Aquaporin water channels (Nobel Lecture), Angew. Chemie Int. Ed. 43 (2004) 4278–4290, https://doi.org/10.1002/anie.200460804.

[35] P. Agre, S. Sasaki, M.J. Chrispeels, Aquaporins: a family of water channel proteins, Am. J. Physiol. Physiol. 265 (1993) F461, https://doi.org/10.1152/ajprenal.1993.265.3.F461.

[36] M. Kumar, M. Grzelakowski, J. Zilles, M. Clark, W. Meier, Highly permeable polymeric membranes based on the incorporation of the functional water channel protein Aquaporin Z, Proc. Natl. Acad. Sci. 104 (2007) 20719 LP – 20724 http://www.pnas.org/content/104/52/20719.abstract.

[37] X. Li, S. Chou, R. Wang, L. Shi, W. Fang, G. Chaitra, C.Y. Tang, J. Torres, X. Hu, A.G. Fane, Nature gives the best solution for desalination: aquaporin-based hollow fiber composite membrane with superior performance, J. Memb. Sci. 494 (2015) 68–77, https://doi.org/10.1016/J.MEMSCI.2015.07.040.

[38] Y. Zhao, C. Qiu, X. Li, A. Vararattanavech, W. Shen, J. Torres, C. Hélix-Nielsen, R. Wang, X. Hu, A.G. Fane, C.Y. Tang, Synthesis of robust and high-performance aquaporin-based biomimetic membranes by interfacial polymerization-membrane preparation and RO performance characterization, J. Memb. Sci. 423–424 (2012) 422–428, https://doi.org/10.1016/j.memsci.2012.08.039.

[39] S. Qi, R. Wang, G.K.M. Chaitra, J. Torres, X. Hu, A.G. Fane, Aquaporin-based biomimetic reverse osmosis membranes: stability and long term performance, J. Memb. Sci. 508 (2016) 94–103, https://doi.org/10.1016/J.MEMSCI.2016.02.013.

[40] C.Y. Tang, Y. Zhao, R. Wang, C. Hélix-Nielsen, A.G. Fane, Desalination by biomimetic aquaporin membranes: review of status and prospects, Desalination 308 (2013) 34–40, https://doi.org/10.1016/j.desal.2012.07.007.

[41] Y. Shen, P.O. Saboe, I.T. Sines, M. Erbakan, M. Kumar, Biomimetic membranes: a review, J. Memb. Sci. 454 (2014) 359–381, https://doi.org/10.1016/J.MEMSCI.2013.12.019.

[42] D. Zahn, T. Frömel, T.P. Knepper, Halogenated methanesulfonic acids: a new class of organic micropollutants in the water cycle, Water Res. 101 (2016) 292–299, https://doi.org/10.1016/j.watres.2016.05.082.

[43] N. Kudo, Y. Kawashima, Toxicity and toxicokinetics of perfluorooctanoic acid in humans and animals, J. Toxicol. Sci. 28 (2003) 49–57, https://doi.org/10.2131/jts.28.49.

[44] W.A. Gebbink, L. van Asseldonk, S.P.J. van Leeuwen, Presence of emerging per- and polyfluoroalkyl substances (PFASs) in river and drinking water near a fluorochemical production plant in the Netherlands, Environ. Sci. Technol. 51 (2017) 11057–11065, https://doi.org/10.1021/acs.est.7b02488.

[45] J.F.M. Versteegh, P. de Voogt, Risicoduiding en vóórkomen van FRD-903 in drinkwater en drinkwaterbronnen bij een selectie van drinkwaterwinningen in Nederland, RIVM Letter Report 2017-0175, 2017, https://doi.org/10.21945/RIVM-2017-0175.

[46] D. Vughs, K.A. Baken, M.M.L. Dingemans, P. de Voogt, The determination of two emerging perfluoroalkyl substances and related halogenated sulfonic acids and their significance for the drinking water supply chain, Environ. Sci. Process. Impacts. 21 (2019) 1899–1907, https://doi.org/10.1039/C9EM00393B.

[47] V. Albergamo, B. Blankert, E.R. Cornelissen, B. Hofs, W.-J. Knibbe, W. van der Meer, P. de Voogt, Removal of polar organic micropollutants by pilot-scale reverse osmosis drinking water treatment, Water Res. 148 (2019) 535–545, https://doi.org/10.1016/j.watres.2018.09.029.

[48] T. Fujioka, S.J. Khan, J.A. McDonald, L.D. Nghiem, Validating the rejection of trace organic chemicals by reverse osmosis membranes using a pilot-scale system, Desalination 358 (2015) 18–26, https://doi.org/10.1016/j.desal.2014.11.033.

[49] V. Yangali-Quintanilla, S.K. Maeng, T. Fujioka, M. Kennedy, G. Amy, Proposing nanofiltration as acceptable barrier for organic contaminants in water reuse, J. Memb. Sci. 362 (2010) 334–345, https://doi.org/10.1016/j.memsci.2010.06.058.

[50] T. Fujioka, L.D. Nghiem, Modification of a polyamide reverse osmosis membrane by heat treatment for enhanced fouling resistance, Water Sci. Technol. Water Supply 13 (2013) 1553–1559 http://ws.iwaponline.com/content/13/6/1553.abstract.

[51] R. Loos, G. Locoro, S. Comero, S. Contini, D. Schwesig, F. Werres, P. Balsaa, O. Gans, S. Weiss, L. Blaha, M. Bolchi, B.M. Gawlik, Pan-European survey on the occurrence of selected polar organic persistent pollutants in ground water, Water Res. 44 (2010) 4115–4126, https://doi.org/10.1016/j.watres.2010.05.032.

[52] R. Loos, B.M. Gawlik, G. Locoro, E. Rimaviciute, S. Contini, G. Bidoglio, EU-wide survey of polar organic persistent pollutants in European river waters, Environ. Pollut. 157 (2009) 561–568, https://doi.org/10.1016/j.envpol.2008.09.020.

[53] T. Fujioka, L.D. Nghiem, S.J. Khan, J.A. McDonald, Y. Poussade, J.E. Drewes, Effects of feed solution characteristics on the rejection of N-nitrosamines by reverse osmosis membranes, J. Memb. Sci. 409 (2012) 66–74, https://doi.org/10.1016/j.memsci.2012.03.035.

[54] A.R.D. Verliefde, E.R. Cornelissen, S.G.J. Heijman, J.Q.J.C. Verberk, G.L. Amy, B. Van der Bruggen, J.C. van Dijk, Construction and validation of a full-scale model for rejection of organic micropollutants by NF membranes, J. Memb. Sci. 339 (2009) 10–20, https://doi.org/10.1016/j.memsci.2009.03.038.

[55] V. Albergamo, R. Helmus, P. de Voogt, Direct injection analysis of polar micropollutants in natural drinking water sources with biphenyl liquid chromatography

coupled to high-resolution time-of-flight mass spectrometry, J. Chromatogr. A 1596 (2018) 53–61, https://doi.org/10.1016/j.chroma.2018.07.036.

[56] L.G. Dijkhuis, Hydrochemisch onderzoek Kamerik - Eindrapport, Oasen Intern. Rep. (1998).

[57] C.Y. Tang, Y.-N. Kwon, J.O. Leckie, Fouling of reverse osmosis and nanofiltration membranes by humic acid—effects of solution composition and hydrodynamic conditions, J. Memb. Sci. 290 (2007) 86–94, https://doi.org/10.1016/j.memsci.2006.12.017.

[58] K.O. Agenson, T. Urase, Change in membrane performance due to organic fouling in nanofiltration (NF)/reverse osmosis (RO) applications, Sep. Purif. Technol. 55 (2007) 147–156, https://doi.org/10.1016/j.seppur.2006.11.010.

[59] T. Fujioka, S.J. Khan, J.A. McDonald, R.K. Henderson, Y. Poussade, J.E. Drewes, L.D. Nghiem, Effects of membrane fouling on N-nitrosamine rejection by nanofiltration and reverse osmosis membranes, J. Memb. Sci. 427 (2013) 311–319, https://doi.org/10.1016/j.memsci.2012.09.055.

[60] J.E. Drewes, C. Bellona, M. Oedekoven, P. Xu, T.-U. Kim, G. Amy, Rejection of wastewater-derived micropollutants in high-pressure membrane applications leading to indirect potable reuse, Environ. Prog. 24 (2005) 400–409, https://doi.org/10.1002/ep.10110.

[61] K. Kimura, S. Toshima, G. Amy, Y. Watanabe, Rejection of neutral endocrine disrupting compounds (EDCs) and pharmaceutical active compounds (PhACs) by RO membranes, J. Memb. Sci. 245 (2004) 71–78, https://doi.org/10.1016/j.memsci.2004.07.018.

[62] A.M. Comerton, R.C. Andrews, D.M. Bagley, C. Hao, The rejection of endocrine disrupting and pharmaceutically active compounds by NF and RO membranes as a function of compound and water matrix properties, J. Memb. Sci. 313 (2008) 323–335, https://doi.org/10.1016/j.memsci.2008.01.021.

[63] A.R. Loiola, J.C.R.A. Andrade, J.M. Sasaki, L.R.D. da Silva, Structural analysis of zeolite NaA synthesized by a cost-effective hydrothermal method using kaolin and its use as water softener, J. Colloid Interface Sci. 367 (2012) 34–39, https://doi.org/10.1016/j.jcis.2010.11.026.

[64] T. Hoang, G. Stevens, S. Kentish, The effect of feed pH on the performance of a reverse osmosis membrane, Desalination 261 (2010) 99–103, https://doi.org/10.1016/j.desal.2010.05.024.

[65] T. Fujioka, S.J. Khan, J.A. McDonald, L.D. Nghiem, Rejection of trace organic chemicals by a hollow fibre cellulose triacetate reverse osmosis membrane, Desalination 368 (2015) 69–75, https://doi.org/10.1016/j.desal.2014.06.011.

[66] I. Kocsis, Z. Sun, Y.M. Legrand, M. Barboiu, Artificial water channels—deconvolution of natural Aquaporins through synthetic design, Npj Clean Water 1 (2018) 13, https://doi.org/10.1038/s41545-018-0013-y.

[67] T. Henzler, Q. YE, E. Steudle, Oxidative gating of water channels (aquaporins) in Chara by hydroxyl radicals, Plant Cell Environ. 27 (2004) 1184–1195, https://doi.org/10.1111/j.1365-3040.2004.01226.x.

[68] N. Uehlein, K. Fileschi, M. Eckert, G.P. Bienert, A. Bertl, R. Kaldenhoff, Arbuscular mycorrhizal symbiosis and plant aquaporin expression, Phytochemistry 68 (2007) 122–129, https://doi.org/10.1016/j.phytochem.2006.09.033.

[69] M. Xie, W. Luo, H. Guo, L.D. Nghiem, C.Y. Tang, S.R. Gray, Trace organic contaminant rejection by aquaporin forward osmosis membrane: transport mechanisms and membrane stability, Water Res. 132 (2018) 90–98, https://doi.org/10.1016/j.watres.2017.12.072.

[70] S.-K. Kam, J. Gregory, The interaction of humic substances with cationic polyelectrolytes, Water Res. 35 (2001) 3557–3566, https://doi.org/10.1016/S0043-1354(01)00092-6.